



## DIGITAL ACOUSTIC MODEM DESIGN FOR NARROWBAND UNDERWATER VEHICLE COMMUNICATIONS

Ertan Uysal

*AirTies Wireless Networks, Software Engineer, İstanbul, Turkey*

Serhat Yılma

*Department of Electronics and Telecommunications Engineering, Kocaeli University, Kocaeli, Turkey,  
serhatyilmaz@ieee.org*

Murat Kuzlu

*Electrical Engineering Technology, Old Dominion University, Norfolk, Virginia, USA.*

Follow this and additional works at: <https://jmstt.ntou.edu.tw/journal>



Part of the [Engineering Commons](#)

### Recommended Citation

Uysal, Ertan; Yılma, Serhat; and Kuzlu, Murat (2018) "DIGITAL ACOUSTIC MODEM DESIGN FOR NARROWBAND UNDERWATER VEHICLE COMMUNICATIONS," *Journal of Marine Science and Technology*: Vol. 26: Iss. 4, Article 12.

DOI: 10.6119/JMST.201808\_26(4).0012

Available at: <https://jmstt.ntou.edu.tw/journal/vol26/iss4/12>

This Research Article is brought to you for free and open access by Journal of Marine Science and Technology. It has been accepted for inclusion in Journal of Marine Science and Technology by an authorized editor of Journal of Marine Science and Technology.

---

# DIGITAL ACOUSTIC MODEM DESIGN FOR NARROWBAND UNDERWATER VEHICLE COMMUNICATIONS

## Acknowledgements

This manuscript was edited by Wallace Academic Editing

# DIGITAL ACOUSTIC MODEM DESIGN FOR NARROWBAND UNDERWATER VEHICLE COMMUNICATIONS

Ertan Uysal<sup>1</sup>, Serhat Yılmaz<sup>2</sup>, and Murat Kuzlu<sup>3</sup>

Key words: acoustics, coding, underwater vehicle communication.

## ABSTRACT

Underwater communication has become a crucial data transmission technology for commercial and military marine applications in the last few decades. However, most underwater communication applications still use analogue technologies. Recent advances in digital signal processing technology have enabled numerous applications in different fields, especially in underwater wireless communications. This paper presents a digital underwater communication system, which transmits and receives acoustic signals via hydrophones employed as acoustic transmitters and receiver units. In this study, coding and modulation methods were also implemented in the prototype through a series of simulations.

## I. INTRODUCTION

Over the past several decades, the investigation and improvement of underwater acoustics on multiuser communications, efficient signal-processing algorithms under interference conditions, and novel, effective schemes for both encoding and modulation have increased considerably (Stojanovic, 1996). It is essential to research how acoustic modems could be developed to provide the maximum transmission range and data transfer rates. This is because the acoustic channel underwater is not constant; the transmission can vary according to environmental factors such as the salinity, depth, seaweed content, and temperature of the water (Sendra et al., 2016). Wireless communication for underwater applications is crucial for many applications, such as the transmission of speech, oil exploration, environmental pollution, and wildlife monitoring, as well as the collection of scientific

information from stations at the bottom of the ocean and from remotely operated vehicles (ROVs). The effectiveness of digital acoustic communication systems has enabled the development of such applications (Singer et al., 2009). Autonomous underwater vehicles determine and control their positions using digital sonar, as the global positioning system (GPS) is unavailable in underwater environments (Yuh and Nie, 2000).

The first modern underwater communication system (UCS) for submarines in the United States, developed in the 1940s, was an underwater telephone. The device utilised amplitude modulation (AM) on the 811 KHz carrier frequency range. The primary reason for using an acoustic carrier is the low acoustic energy and electromagnetic losses in seawater. Therefore, acoustic radiation is more suitable than an electromagnetic carrier. Optical waves are subject to scattering, and a reasonable level of accuracy is required during laser-beam targeting. An acoustic channel has a narrow bandwidth, which often results in signal scattering in both the time and frequency domain (Hwei, 1995). To overcome the limitations of certain methods, including orthogonal frequency division multiplexing (OFDM) and compressed sensing, underwater acoustic transmissions are necessary (Lei et al., 2008; Fazel et al., 2010; Lu et al., 2013). Zhiqiang et al. (2010) suggested using an electric current for an underwater modem at a 1 Mbps data rate. Yagnamurthy and Jelinek (2013) designed a cost-effective underwater communication radio system that could perform complete audio digital signal processing (DSP). Benson et al. (2010) compared several UCSs in terms of data rate, transmission distance, transmitter/receiver power, and cost. The hydrophone (i.e., transducer) is the most critical component from a cost perspective for underwater communication applications.

Various techniques can be used to design an underwater communications system that overcomes the effects of multipath and Doppler spreads as well as phase variations in the underwater environment. These techniques, including the choice of modulation (quadrature AM [QAM], frequency-shift keying [FSK], and phase-shift keying [PSK]) and the transmitter/receiver structure, and examples of system designs are summarised in (Stojanovic, 1996). Takinaci and Taralp (2013) developed a propeller noise pattern for training purposes in submarine sonar simulators. Data rates for multicarrier modulation techniques, (i.e., quadrature phase-shift keying [QPSK], and QAM) are evaluated at various

Paper submitted 03/17/17; revised 02/09/18; accepted 06/27/18. Author for correspondence: Serhat Yılmaz (e-mail: serhatyilmaz@ieee.org).

<sup>1</sup> AirTies Wireless Networks, Software Engineer, Istanbul, Turkey.

<sup>2</sup> Department of Electronics and Telecommunications Engineering, Kocaeli University, Kocaeli, Turkey.

<sup>3</sup> Electrical Engineering Technology, Old Dominion University, Norfolk, Virginia, USA.

underwater depths, (e.g., 0.45, 1, and 2 km). Noncoherent modulation methods for applications with low data rates are still in use for underwater communication, whereas coherent modulation schemes are utilised for applications with high data rates (Melodia et al., 2013). Hydrodynamic coefficients of complex-shaped ROVs could be determined using computer aided design, mathematical modelling, and simulation methods (You et al., 2014). Interactions between moving objects and fluid can be extracted by interpolation and meshing techniques, allowing the trajectory of a moving body to be predicted.

Delay uncertainties in acoustic systems disturb the performance of underwater communications. The decomposition of delay into components and analysis of the each component's features allows a reduction in delay uncertainties (Luo et al., 2017).

This paper presents details of the design and implementation of a DSP-based high precision, robust, reliable, and cost-effective UCS. DSP cards and other hardware equipment were selected and designed to satisfy underwater communication requirements. Overall DSP programmes, including encoding-decoding and transmitting-receiving software using the Morse coding and double sideband modulation-demodulation methods were developed in C++. The methods were initially simulated in MATLAB. The developed system was designed to function as the communication system of an underwater vehicle, which receives and transmits control signals and sensory information (Yilmaz et al., 2014). The designation flexibility of a communication system has a suitable shape and structure for use in an underwater vehicle. This system could be used, for example, for the remote control of various underwater devices, and data exchanges between underwater instruments and a surface vessel for commercial and military applications with low data rates.

## II. THE ACOUSTIC COMMUNICATION

Electromagnetic transmission is impossible for underwater applications due to a high attenuation of waves in water. Instead, ultrasound is a viable option for UCSs. Analogue techniques have been employed in the majority of solutions for underwater transmission problems in recent years. The main theoretical considerations and a background to the UCS are provided in the rest of the paper.

### 1. Transmission of Acoustic Waves

Mechanical vibrations of pressure in 3D propagating through a gas, liquid, or solid are called a sound. The pressure applied to the medium is related to the particle velocity, medium density, and sound velocity. Another consideration in UCSs is sound intensity ( $I_s$ ), which is defined as acoustic power over unit area. It can be determined by the production of sound pressure with particle velocity.  $I_s$  is measured logarithmically using a reference point, as provided in (1).

$$L_{I_s} = 10 \log \left( \frac{I_s}{I_\gamma} \right) \quad (1)$$

An acoustic transmission loss,  $ATL_{I_s}$  is decreasing in the  $L_{I_s}$  of a sound emitted from a level at the origin  $L_o$  in the course of distance (d).

$$ATL_{I_s} = L_o - 20 \log(d) - \alpha(d-1) \quad (2)$$

Transmission loss occurs as a result of spreading and attenuation. The spherical spreading model is valid when the transmission spreads from an origin to all directions. However, when the sound reaches a boundary, such as the surface or bottom of the ocean, cylindrical spreading occurs. When the wave is enclosed by an item, it cannot be propagated and the transmission fades.

Attenuation or fading is the scattering of energy along the medium. There are two types of attenuation; absorption and scattering or reverberation losses. Sound in motion causes friction, which results in energy loss, known as absorption loss, (AL), and is converted to heat. The loss depends on water temperature and frequency, as presented in (3).

$$AL = 1.0936 \left( \frac{0.1f^2}{1+f^2} + \frac{40f^2}{4100+f^2} \right) R \quad (3)$$

where  $f$  (kHz) is frequency and  $R$  (metre) is the range. A part of acoustic energy is scattered because of discontinuities such as those caused by fish, bubbles, and the upper and lower boundaries of water. Another part of the sound signal, known as reverberation, is returned back to the receiver. Stojanovic (1999) provided information about UCS requirements and channel characteristics. Experimental tests could be performed to compare measured and mathematically calculated values, including transmit voltage response, transducer input voltage, hydrophone received response, and open circuit (output) voltage (Kuzlu et al., 2010a).

### 2. Modulation and Demodulation Methods Employed

Double sideband (DSB) modulation and demodulation performed by filter pairs is critical in UCSs (Brown, 1979). Impulse response,  $h(t)$ , is obtained by devising a low pass filter (LPF), which provides the necessary characteristics of the transition band,  $H(w)$ .

By multiplying the impulse response by a complex sinusoidal angular frequency ( $w_0$ ), real and imaginary coefficients can be obtained. In the frequency analysis, a  $90^\circ$  phase shifting can be observed between impulse and  $Q$  filter responses, whose coefficients are derived from  $L$  coefficients of the prototype LPF as follows (Kuzlu et al., 2010b), with  $t_s$  representing the sampling time.

$$hI(k) = h(k) \cos \left[ \omega_0 \left( k - \frac{L}{2} + \frac{1}{2} \right) t_s \right] \quad (4)$$

$$hQ(k) = h(k) \sin \left[ \omega_0 \left( k - \frac{L}{2} + \frac{1}{2} \right) t_s \right] \quad (5)$$

3. Encoding

Information on the carrier should be encoded and decoded before sending and after being received, respectively. One of the most popular underwater character transmissions depends on standardised signalling with short and long sound tones in a series, known as Morse code (MC). Time series of MC signalling are initially separated into time series of tone  $n_T(k)$  and silence  $n_S(k)$ , and are traced according to their intervals at the decoding side (Lou and Hsieh, 1999).

MC is an adequately optimised, reliable, and universal coding-encoding protocol. Using this method, it is easy to filter out background noise and sense even weak MC signals, making it an ideal platform for high noise and low signal environments (Lou and Hsieh, 1999). It is an efficient method for controlling a tone to extend the range of a transmission and mitigate interference or signal loss (Hunt and Hunt, 1995). MC has a short bandwidth, allowing small transmitters to send highly effective signals. For this reason, navigation beacons still use MC to identify themselves (Shaw and Lopato, 2014). Furthermore, MC signals transmitted by an underwater vehicle can be encoded by humans after demodulation.

Gray code is a coding-encoding method that searches for a single digit diverging by 1 between sequential numbers of an array. To translate a digital number array such as  $a_1, a_2, a_3, \dots, a_{n-1}, a_n$  to a Gray code  $gry_1, gry_2, gry_3, \dots, gry_{n-1}, gry_n$ , one should start from the last digit  $a_n$  (Gao et al., 2017). If  $a_{n-1}$  is 1, then  $a_n$  should be replaced with  $1 - a_n$ . Otherwise, it should not be changed. The conversion will continue until  $a_1$  is reached. Conversion of a Gray code to a binary number starts with  $gry_n$ , as follows;

$$\sum_n = \sum_{i=1}^{n-1} gry_i \pmod{2}$$

If  $\sum_n = 1$  then  $gry_n$  should be replaced with  $1 - gry_n$ . Otherwise, the previous value should be kept. The next stage continues as follows;

$$\sum_{n-1} = \sum_{i=1}^{n-2} gry_i \pmod{2}$$

Using this approach, corresponding binary conversion is achieved:  $a_1, a_2, a_3, \dots, a_{n-1}, a_n$ .

The main purpose of designing this prototype digital acoustic modem is to provide basic data communication between underwater vehicles and surface terminals. The data usually consists of set and actual values of depth, pitch, yaw, roll, and on-off information of the power led and camera (Hagmann, 2009). MC is one of the preferred communication methods for sending and receiving information with low data rates in the underwater communication environment because of its simplicity and narrow bandwidth use. This reduces overall equipment requirements while satisfying the transmission demands and simplifying the modelling and testing of complex-shaped ROVs. For example, Gray code is principally effective at detecting changes in mono-

Table 1. Comparison of encoding methods in communication.

Specifications	Morse Code	Gray Code
Required Bandwidth	Narrow	Broad
Data Transmission Rate	Low	High
Design Complexity	Simple	Complex
Signal type preferable for transmission	No restriction	Restricted with monotonous changed signals
Noise Tolerance	High	Low
Manually Decoding in the Receiver Side	Possible	Not practical

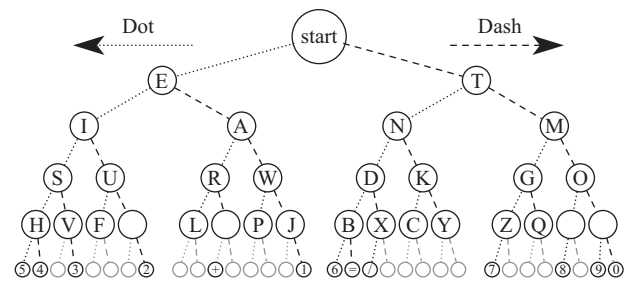


Fig. 1. Binary MC Tree.

tonous data transmissions, where the code senses if one bit or more is changed or not. However, our transmission data structure, in general, is neither sequential nor incremental. For this reason, although several stable coding-encoding methods exist, considering the general duty demands of the remote control of vehicles, MC was employed (Table 1)

International MC depends on five signals. The main two tone signals are: a one-unit-long mark (·) symbolised by a dot and a three-unit-long mark (-) represented by a dash. The three silence signals are: a one-unit-long intracharacter gap, a three-unit-long intraletter gap, and a seven-unit-long intraword gap. For instance, the popular international distress signal, '... --- ...', is an MC representation of SOS (save our souls). Similarly, '... -- ...', represents SMS (short message service) in cell phones. An MC serial could be easily encoded as an MC tree, as shown in Fig. 1.

III. UNDERWATER COMMUNICATION SYSTEM

In this section, design stages of a UCS, including the operation principles of modules, are described. The transmission power in the system is approximately 100 W, and the operating frequency is between 9 KHz and 40 KHz.

1. Hardware Description of the Transmitter and Receiver

The system can be discussed under two headings: the transmitter and receiver. The block diagram of the designed system is given in Fig. 2.

The transmitting input value is entered on the 8-bit keypad on the main board. A C++ based software unit, prepared in the Code Composer Studio (CCS) environment (Texas Instruments

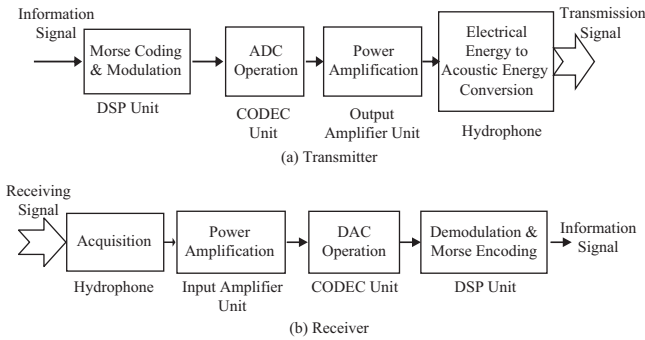


Fig. 2. Block diagram of the UCS.

Inc. (TI, USA), encodes the values to MC data. The encoded signal is modulated with DSB amplitude modulation. The adjustable carrier frequency is set to 8087.5 Hz, which is defined in the STANAG 1074 standard for underwater communication. Encoded and modulated signals are sent to the analogue to digital converter ADC unit. A built-in module DSP card is used for sampling and generating audio signals. These processes are performed by an integrated sound codec module. Through this module, the high quality conversion of sound to digital signals as well as modulating and demodulating processes are performed precisely.

The output amplifier unit amplifies the codec output signal, and then this analogue signal is sent using a B & K 8103 hydrophone (Bruel & Kjaer Inc., Nærum, Denmark) in a test pool. The modulated signal is received by the hydrophone receivers, amplified, and sent to the line-in of an AIC23 codec, which is a high-performance stereo audio codec with highly integrated analogue functionality, to be convert into a digital signal. The digital signal is mixed by the carrier signal obtained using amplitude modulation with envelope detection. Finally, an encoded software unit encodes the demodulated digital value.

2. Input Amplifier (Receiver)

The modulated signal received by the hydrophone receiver has a very low voltage level (in microvolts). This signal should be augmented to process it in DSP. In this design, the received signal is amplified by a preamplifier approximately 60 times its original value as illustrated in Fig. 3. The preamplifier consists of two gain modules: a transformer and a low-power buffer amplifier. First, the transformer is used to amplify the signal by 20 times its original value. Then, the low-power buffer amplifier increases the signal amplitude three-fold and cancels the noise caused by the underwater environment.

3. Output Amplifier (Transmitter)

The codec signal output is at the millivolt level (maximum 1  $V_{rms}$ ); this level is not sufficient to send long distance communication signals in seawater. For this reason, the modulated signal should be amplified. In this design, an output amplifier unit amplifies the codec output (coded and modulated) signal approximately 150-fold. It consists of three amplifier units: operational and power amplifiers as well as a transformer. Operational and

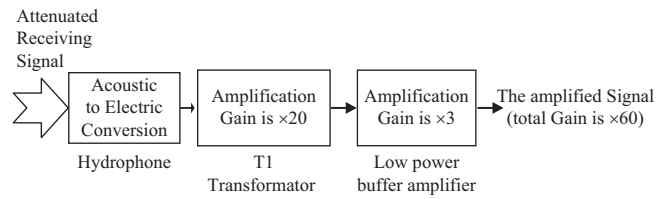


Fig. 3. Block diagram of input amplification.

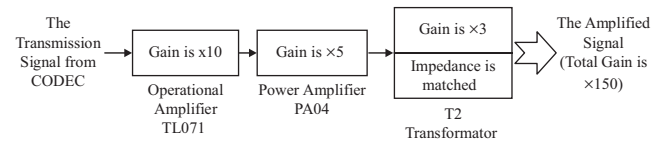


Fig. 4. Block diagram of the output amplification.

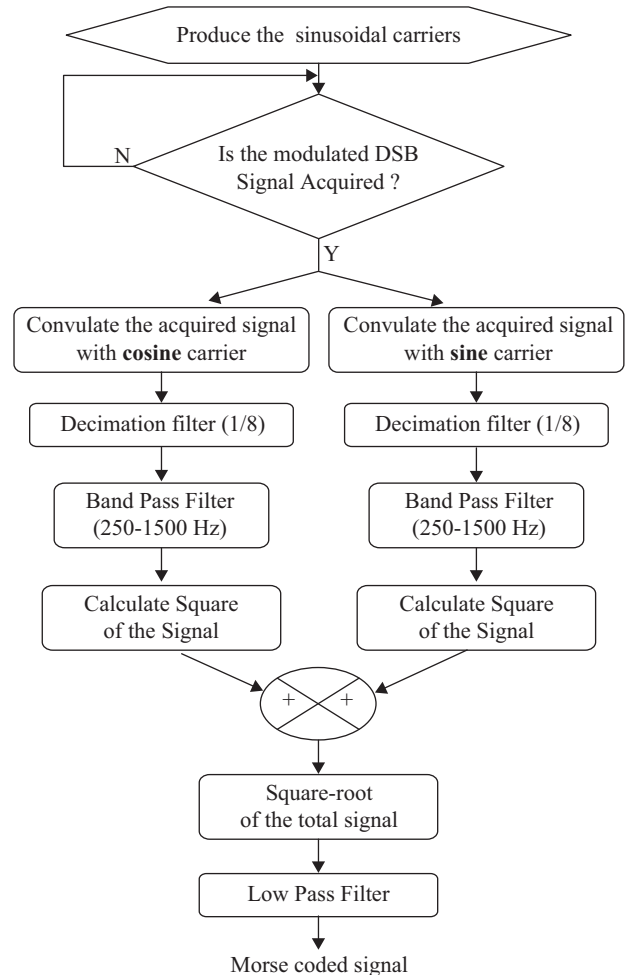


Fig. 5. Demodulation of the DSB signal.

power amplifiers were selected to amplify the low-level signal of the codec output according to the selected DSP specification. The signal is amplified 50-fold by these amplifiers. Then, the signal is reamplified three times by a transformer for impedance

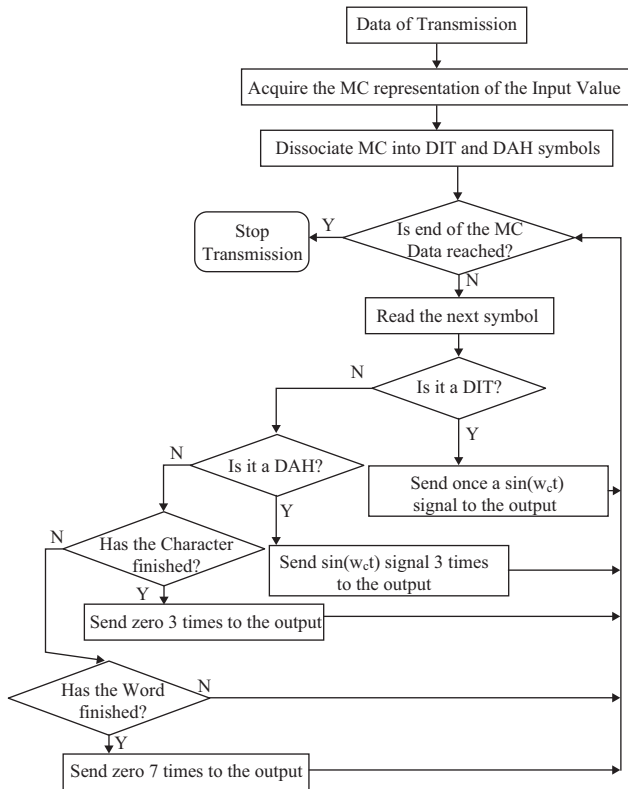


Fig. 6. MC DSB algorithm.

matching with the main board. Thereafter, the amplified analogue signal is sent by the B & K 8103 hydrophone into a test pool (see Fig. 4).

4. Software Description

The UCS system software is composed of modulation/demodulation and Morse encoding/decoding algorithms.

Amplitude Demodulation with an Envelope Detection Algorithm

Following the ADC conversion, a digital signal is mixed by the carrier signal obtained using amplitude modulation with envelope detection. Frequency decimation, band pass filter, and LPF processes are applied, as shown in Fig. 5. The final digital signal is encoded by means of the MC-encoded software unit.

Coded DSB Modulation Algorithm

Fig. 6 illustrates the MC DSB modulation algorithm. The transmitting input value is entered via the 8-bit keypad on the main board. The software extracts the MC equivalent of the input value. The value is then separated into ‘DIT and DAH’ signals (Lou and Hsieh, 1999) according to the MC value table. A loop is started from zero to the MC data length and at this point;

- (1) If the character has the DIT Signal, then a  $\sin(w_c t)$  is sent to the output once
- (2) If the character has the DAH Signal, then a  $\sin(w_c t)$  is sent to the output three times

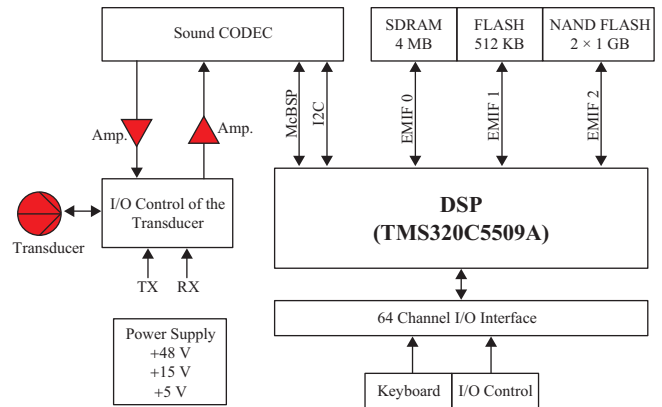


Fig. 7. Designed DSP card.

- (3) If the letter signal has ended, a zero is sent to the output three times
- (4) If the word signal has ended, a zero is sent to output three times

The methods were initially simulated in MATLAB.

5. Hardware and Software of the Prototype DSP Cards

The structure of the designed DSP card is illustrated in Fig. 7. This structure consists of a DSP, sound codec, memory units (i.e., synchronous dynamic RAM, flash, and NAND flash), a 64-channel I/O interface, and a power supply. The DSP is the key component of the system. It is responsible for processing the signal received from the sound codec. Synchronous dynamic RAM (SDRAM) is memory that is synchronised with the system bus. The flash memory is used for DSP source code storage, whereas NAND flash memory is used to record the received/transmitted data if required for further applications. The I/O interface is used to access the keypad and control the warning and notification light-emitting diodes. Finally, the power supply is responsible for providing the power requirements to the UCS, (i.e., +5 V for DSP and other integrated circuits, +15 V for operational amplifiers, and +48 V for the power amplifier).

Software architecture design of the system from low to high levels is provided in Fig. 8. This architecture consists of four layers: (1) transceiver, receiver, and test modules, (2) signal processing library, (3) DSP basic input/output system (BIOS) processing system and Chip Support Libraries, and (4) DSP (TMS320C5509A). The UCS software is written in C++ in the Code Composer Studio (CCS) environment, which was provided by TI (USA). Transceiver, receiver, and test modules were developed for internal, user interface, MC, and signal processing.

The signal processing library is provided by TI for CCS environments. It includes fast Fourier transform, filter functions, correlation and convolution functions, and magnitude and angle operations. The DSP (BIOS) and CSL provided by TI enable an application programming interface (API) for configuring and controlling the DSP on-chip peripherals. DSP (TMS320C5509A, TI Inc., USA) refers to the selected DSP hardware.



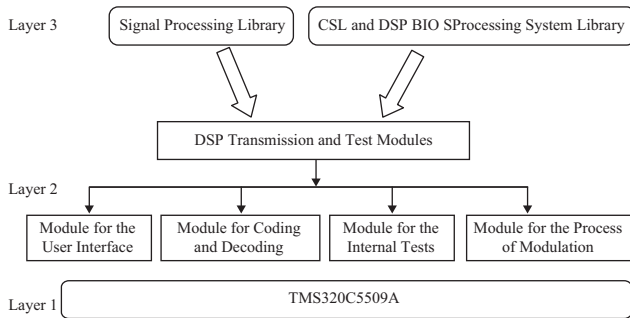


Fig. 8. Structure of the system's DSP programme.

Table 2. Underwater communication subsystems.

Sub Unit	Pcs	Description
Power Supply	1	$\pm 48$ V, $\pm 15$ V, 5 V isolated power supply
DSP Card	2	Digital signal processing, microcontroller processes card
Main Board	2	Connection card between User, DSP Card, Amplifier card
Amplifier Card	1	Amplifier card for amplifying the sound signal
Hydrophone	2	Transmitter and receiver unit underwater
Water Tank	1	A tank filled up with water

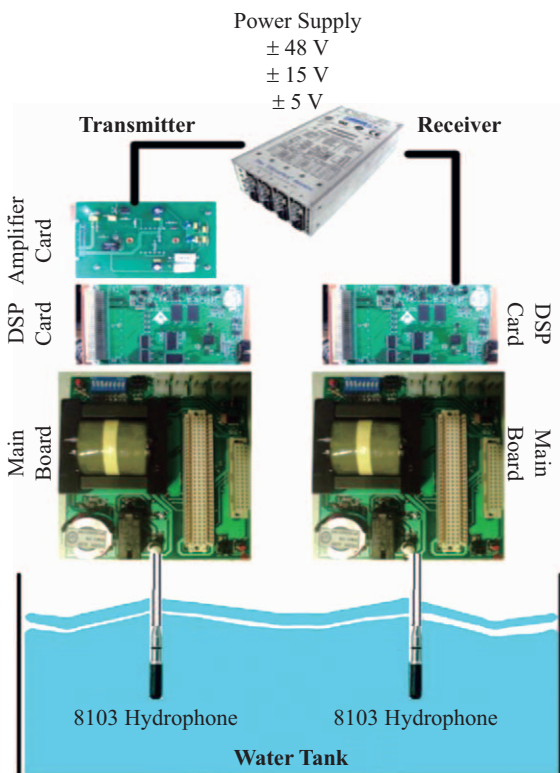


Fig. 9. Underwater communication system.

## 6. Prototype Underwater Communication System

The prototype UCS for underwater acoustic communication and its units are illustrated in Fig. 9, and their utilities are provided in Table 2. Omnidirectional hydrophones are used on both the receiver and transmitter sides in this implementation. Transmitter and receiver units are identical, except that the transmitter unit contains a power amplifier unit. These units contain the DSP card for signal processing, main board for the I/O interface and operational amplifiers, hydrophone for sending and receiving analogue signals, and power supply.

The power amplifier unit is required for only the transmitter unit. This is because the transmitter unit requires an extra power amplifier for long distance communications.

The interface and dimensions of the card were designed to be compatible with the testing underwater vehicle provided by



Fig. 10. Underwater vehicle provided by Kocaeli University (Yilmaz et al., 2014).

Kocaeli University (Yilmaz et al., 2014). Although this study mainly focused on the design of the modems, the application area can offer a feasibility analysis in terms of the data length and structure that can be transmitted and received.

## IV. FEASIBILITY ANALYSIS OF THE DATA TRANSMISSION RATES

The sufficiency of the acoustic modem rates on sending fundamental commands and receiving data related to underwater vehicles is a crucial concern.

To aid in the development of control methods in underwater vehicle technologies, an underwater test platform composed of an experimental tank that can produce distortion effects, and an underwater vehicle that can perform dynamic control under these effects were prepared in the laboratories of Kocaeli University, Engineering Faculty, Department of Electronics and Telecommunications. The platform allows the testing of novel methods and designs for handling communication and control applications under the effects of distortion. The platform enables students to test their projects regarding sensorial applications, signal processing, microcontroller and software programming, new developments on control and communication methods, and software and electronic card designs (Fig. 11(a)).

The methods for the desired movements are handled and processed in the control program interface (CPI) (Fig. 11(b)). The vehicle is remotely operated through a cable. Temporarily, an acoustic modem is fitted onto the vehicle and joined to the



**Table 3. Data Structure Received by the CPI.**

Start	E-Compass	ID	Controller	Temp. (°C)
1 Byte	12 Bytes	1 Byte	2 Bytes	2 Bytes
Acceleration	On-off Key	ADC	Stop	
6 Bytes	1 Byte	8 Bytes	1 Byte	

**Table 4. Data structure sent by the computer interface.**

Starting	Control	Max Pressure	Reference	ID2
1 Byte	1 Byte	1 Byte	12 Bytes	1 Byte
PID Control	ID3	Movement	On-off key	Stop
12 Bytes	1 Byte	1 Byte	1 Byte	1 Byte

**Table 5. Reference data structure.**

Yaw	Roll	Depth
4 Bytes	4 Bytes	4 Bytes

controller card for testing purposes. The stability of the vehicle is reset using floats.

**1. Receiving Data Structure from the Vehicle**

The data received from the vehicle control card and monitored on the computer store the status information of the vehicle. These data are from the electronic compass, temperature gauge, acceleration, the on-off status of the lights and camera, and ADC output of the pressure sensor that monitors the depth variable and controller output (in terms of pulse with modulation). The received data had a length of 34 bytes including start, stop, and verification bytes. The receiving data sequence is provided in Table 3.

**2. Sending Data Structure to Vehicle**

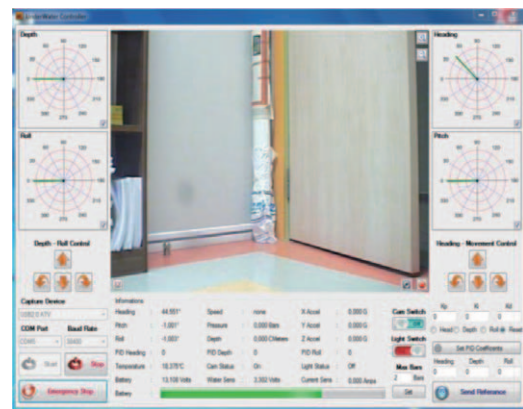
The data sent from CPI to the vehicle includes information of vehicle control. This information is composed of data related to starting the control process, reference setting values, control data, forward or backward movement data, and lighting and camera on-off data. The sent data was 32 bytes, including start, stop, and identity (ID) bytes. The received data sequence is provided in Table 4.

The reference data includes three yaw, roll, and depth values for the vehicle. Each of the reference values is 4 bytes long, as presented in Table 5.

In conclusion, when the full control demands of the vehicle are analysed, approximately 34 bytes are required. The current rate of the designed modems was 4 bit/s (16 bit/ 4 s). Targets could be achieved by adjusting variables or structural changes being made to the card (Table 6). However, these amendments could result in disadvantages. The critical problem in the control process is the refresh time. Commands and reference values do not change rapidly in an underwater orientation mission. Thus, control of the movements in depth or in Euler Rotations of the vehicle, could be realised using the control card.



(a)



(b)

**Fig. 11. (a) UV Test Platform, (b) CPI of the Test Platform (Yilmaz et al., 2014).**

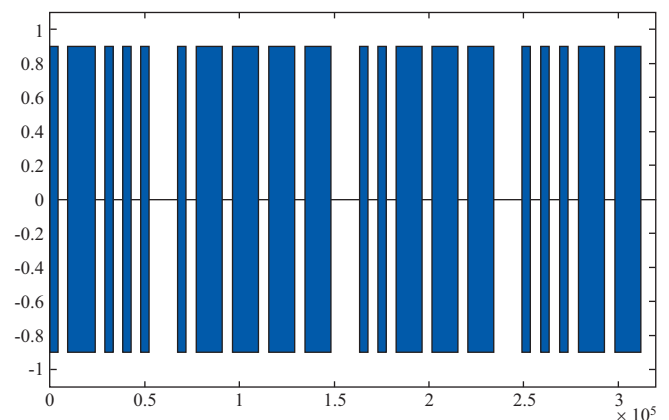


**Fig. 12. Output Signal of the sound card produced by MATLAB Code.**

**V. RESULTS AND DISCUSSION**

In this study, the prototype design of a pair of digital acoustic modems was realised and the acoustic signal transmission was observed underwater. DSB modulation and amplitude demo-

**Table 6. Suggestions on trade-offs between the transmission data and modem rate.**

Suggested Improvements		Probable Inherent Disadvantages
Adjustment on variables	Frequency of the sinusoidal signal could be increased. In this way period of the signal will be shortened.	Binary Codes (0-1) could be confused
	Signal quantisation level could be carried from 0-1 (1 Bit) to 0-32 (4 Bit).	Signal could be affected more from attenuations.
	In the first stage, simply a 4 byte depth control without parity checks could be realised. The MC DSB algorithm itself has already checking measures.	This will suspend other activities such as roll and yaw control.
Structural Changes	Control Card of the Underwater Vehicle includes a Beagle Bone Development Card (1 GHz Sitara AM3359 ARM Cortex-A8 Processor) and an ARM Cortex-M4F based STM32F407VGT6 microprocessor (168 MHz). Both of the processors could hold control applications. There is no need to control from CPI. CPI could send basic commands such as lighting on-off, ADC start and sending new reference values due to a new mission. Mission does not change in seconds. It is rather change in minutes. In these periods the vehicle could autonomously control by its processors.	The main aim of the wireless communication is releasing underwater vehicle alone and bring about a semi autonomy rather than ROV. This situation is relevant for the main purpose. However, online observation and plotting the navigation of UV onshore will be restricted with minutes.



**Fig. 13. Transmitter output signals (blue: codec output, pink: amplifier card output, green: main board output).**



**Fig. 14. Receiver’s received signal.**

dulation with the envelope detection method were successfully performed. Applying the capabilities of MATLAB into the sound cards can be utilised for the production and encoding of MC test signals (Shao, 2010).

In our study, a transceiver signal was initially produced in MATLAB. Fig. 12 presents the monitoring of signals generated using MATLAB for ‘& 123’ data. Generated data were encoded as .-... (&), ---- (1), ..--- (2) and ...-- (3).

Output signals at the transmitting side are shown in Fig. 13. The codec output maximum gain is nearly  $\pm 10$  mV (shown in blue), whereas the amplifier card output is nearly  $\pm 10$  V (shown in pink). The main board output transferred to the hydrophone is nearly  $\pm 30$  V (shown in green). The performance of a UCS mainly depends the selected hydrophone’s receiver and transmitter sensitivities. The transmitter sensitivity is the measured pressure output of a hydrophone for an input of 1 Vrms (i.e., root mean square voltage value at a distance of 1 m away from the projector), whereas the receiver sensitivity is the measured open circuit Vrms at the hydrophone terminals. Various acoustic hydrophones for underwater communication applications are currently available, and are detailed in (Hagmann, 2009).

Fifty test signals were sent and received in a test pool, which is the acoustically isolated open test tank with dimensions of  $15 \times 10 \times 7.5$  m<sup>3</sup>. The input signal at the receiving side is shown in Fig. 14. The received signal is almost  $\pm 10$  mV at a distance of 1 m, and  $\pm 6$  mV at 6 m. High capacitive effect of the existing hydrophone resulted to an ineffective communication. High capacitive effect of the existing hydrophone resulted to an ineffective communication. To obtain a communication for long distances (i.e., 1-10 km), a hydrophone should exhibit low input impedance, known resonance frequency and almost no capacitive and inductive effects at the resonant frequency.

In addition, experimental outcomes were analysed in terms of theoretical results. The sensitivity and power of a transmitter in the related frequencies are factors in the transmission and receiving responses. The reference value was 1 V. The power was dependent on the gains of the amplifiers.

Measurements from the pool tests and theoretical estimations are provided with necessary parameters in the Table A1 according to distance and input voltage of the transducers (Uysal, 2010).

In the transmitter side, TVR (transmission voltage response),  $V_{rms}$  (transducer hydrophone input voltage), and  $P_e$  (logarithmic

**Table 7. Actual (a) and predicted (p) SL and IL values at 1 m and 6 m for 8KHz test signal.**

(dB)		<i>a</i>	<i>p</i>
1 m	SL	169.5424	166.990
	IL	166.990	169.5424
6 m	SL	169.5424	172.095
	IL	156.532	153.979

power efficiency rate of the hydrophone) were measured as 140 dB re 1  $\mu$ Pa-m/V, 30 V, and  $20 \log (\%100) = 0$ , respectively. As a function of these parameters, the actual hydrophone source level (aSL) value of the measurement is calculated in (6).

$$aSL = TVR + 20 \log(V_{rms}) + P_e \quad (6)$$

Additionally, pIL refers to the predicted value of the intensity level at  $r$  m. away from the transmitter side. The theoretical prediction refers to the model of transmission loss (TL) (7)

$$pIL = aSL - TL = aSL - 20 \log(r) \quad (7)$$

At the receiver side, the measured actual hydrophone intensity level (aIL) and predicted source level (pSL) refer to the hydrophone output voltage (i.e., output circuit voltage [OCV]) are calculated:

$$aIL = 20 \log(OCV) - RR \quad (8)$$

$$pSL = 20 \log(OCV) + RR + 20 \log(r) \quad (9)$$

These values were calculated when gain levels were not considered. Water pool measurement results for the transmitter-receiver distances of  $r = 1$  m and  $r = 6$  m for 8 KHz are shown in Table 7. The predicted values ( $p$ ) and measured actual values ( $a$ ) of the SL and IL are compared as follows:

Differences between the actual and predicted values increase depending on the signal distance. Because the sound rapidly reached the top and bottom of the pool, at these bounds, the sound did not conform to the spherical spreading model. External non-linear effects such as absorption losses, and scattering because of discontinuities (as mentioned in the Section II on Acoustic Communication) may have resulted in these estimation errors. Definitions and values of critical parameters in the transceiver and receiver sides are provided in Appendix A.

A testing platform on which transmission data for the control process will be used was introduced. Parameters that determine the data length are described. A data length of 34 bytes is required to acquire a signal from an ROV. Moreover, 32 bytes are required to send ROV commands such as start, stop, and ID bytes. The current rate of the designed modems was 4 bit/s. Some adjustments and improvements on the design of the modem were proposed for efficient ROV control. The manoeuvring capability of the underwater vehicle determines its mechanical duty cycle. A prolonged period for control commands is feasible for this duty cycle.

## VI. CONCLUSION

With advanced technologies emerging, DSPs have been used for a wider variety of applications, such as UCSs. In this study, a cost-effective and reliable digital acoustic modem was designed and implemented for underwater applications using MC. The DSB method was employed in the modulation and demodulation of the transmission. The proposed solution provides superior performance over previous analogue technologies. The advantages of DSP were confirmed. Users can simply create filters or implement any control method using the aforementioned software without any changes in hardware.

The designed acoustic modem provides a flexible platform for implementing telecommunication methods (e.g., modulation and demodulation) for various underwater communication applications. Numerous types of underwater vehicle with limited chambers and hydrodynamic shapes can be allocated electronic cards with restricted standard acoustic modem operations. The small size and flexibility of the prototype allows the hardware to be re-designed and the card to be reshaped or integrated with control cards for use in other vehicles such as torpedo-type vehicles. The acoustic signal transmission and receiving capability of the system were analysed in an experimental pool. MC signals successfully reached the target and were then demodulated and decoded by the systems' software. One-hundred percent of the transmitted signals were received and decoded in the 1-m-range and 96% were successfully received and decoded in the 6-m-range. This was caused by transmission loss due to the hydrophone used in the system.

The source level was predicted to be 2.5524 dB lower than the actual SL for a distance of 1 m and 2.5527 dB higher for a distance of 6 m. Similarly, the IL was estimated to be 2.5524 dB higher than the actual IL for a distance of 1 m and 2.5527 dB lower for a distance of 6 m. If it was equipped with more powerful hydrophones, the developed UCS system equipped could be used in high seas. The system will be analysed in terms of the transmission of control signals and sensory information of an underwater vehicle in future studies. For this reason, transmission rates of the designed acoustic modem were analysed in terms of whether it can send fundamental commands and receive data from underwater vehicles. It was revealed that orientation does not change frequently in a mission. Thus, the control process could be realised by the designed acoustic modems.

## ACKNOWLEDGEMENTS

This manuscript was edited by Wallace Academic Editing.

## APPENDIX. A

Table A1. Parameters of the transmission

Parameter	Definition	Value
$RR$	Hydrophone Receiving Response	210.4 dB re 1 V
$G_A$	Gain to frequency of power amplifier	89dB re $\mu\text{Pa}$
$G_{pamp}$	Gain to frequency of pre amplifier	189 (45.52 dB) in datasheet (48.91 dB) observed in the experiments
$V_{rms}$	Transducer input voltage	$\pm 30$ V
$S_{PL}$	Sound pressure level (Calibrator source level)	166 dB re $\mu\text{Pa}$
$V_{Codec}$	Codec Voltage	$0.56 V_{rms}$
$V_{c}dB$	Codec Read Value in dB	-5.03 dB
$G_{Codec}$	Codec Gain	0.33 (-9.54dB)
$TVR$	transmission voltage response	140 dB re 1 $\mu\text{Pa}\cdot\text{m/V}$
$V_{c}dB = G_{pamp} + G_{Codec} + S_{PL} + RR$		

## REFERENCES

- Benson, B., Y. Li, R. Kastner, B. Faunce, K. Domond, D. Kimball and C. Schurgers (2010). Design of a low-cost, underwater acoustic modem for short-range sensor networks. Proceedings of OCEANS 2010 IEEE, Sydney, Australia, 1, 1-9
- Brown, J.L. (1979). On Quadrature Sampling of Bandpass Signals. IEEE T Aerospace and Electronic Systems 3, 366-367.
- Fazel, F., M. Fazel and M. Stojanovic (2010). Random access compressed sensing in underwater acoustic networks. Proc. of Allerton conference on communications, control, and computing. Monticello, IL, USA, 1-7.
- Gao, J., F. Yang and X. Ma. (2017). Indoor positioning system based on visible light communication with gray-coded identification. Proceedings of 13<sup>th</sup> International Wireless Communications and Mobile Computing Conference (IWCMC 2017), Valencia, Spain, 1, 899 – 903.
- Hagmann, E. (2009). Design of a High Speed, Short Range Underwater Communication System, Semester-Thesis, Swiss Federal Institute of Technology, Zurich, Switzerland, unpublished.
- Hunt, P. C. and L. R. Hunt (1995). Using ultra narrow bandwidth to overcome traditional problems with distribution line carrier. Proceeding of Rural Electric Power Conference, Nashville, Tennessee., USA, D3/1 - D3/8.
- Hwei, P. (1995). Theory and problems of signals and systems. 4th ed. The McGraw-Hill Companies, New York.
- Kuzlu, M., H. Dinçer and S. Öztürk (2010a). DSP Implementation of Underwater Communication Using SSB Modulation with Random Carrier Frequencies. Scientific Research and Essays 5, 1084-1099.
- Kuzlu, M., H. Dinçer, S. Öztürk and T. Kadioglu (2010b). Real time implementation of digital band pass analytic filter pair. Proceeding of IEEE Electrical, Electronics and Computer Engineering Conference, Bursa, Turkey, 626-629.
- Lei, K., X. Z. Yan, J. Han and J. Huang (2008). Design and implementation of underwater OFDM acoustic communication transmitter. Proceeding of ICALIP 2008 International Conference on Audio, Language and Image Processing, Shanghai, Republic of China, 609-613.
- Lou, C. H. and M. C. Hsieh (1999). Automatic morse code recognition with adaptive variable-ratio threshold prediction for physically impaired persons. Proceeding of The First Joint BMES/EMBS Conference Serving Humanity, Advancing Technology, Atlanta, GA, USA, 665.
- Lu, W., Y. Liu and D. Wang (2013). Efficient feedback scheme based on compressed sensing in MIMO wireless networks. Computers and Electrical Engineering 39, 1587-1600.
- Luo, Y., L. Pu, Y. Zhao and J.-H. Cui (2017). Exploring uncertainties of transmission, reception delays for underwater acoustic networks. IEEE Wireless Communications Letters 6(3), 418-421.
- Melodia, T., H. Kulhandjian, L. C. Kuo and E. Demirors (2013). Advances in underwater acoustic networking. In: Mobile Ad Hoc Networking: Cutting Edge Directions, Chapter 23, Second Edition, edited by Basagni, S., M. Conti, S. Giordano and I. Stojmenovic, The Institute of Electrical and Electronics Engineers, John Wiley & Sons, Inc. Publishing, New York, 804-852.
- Sendra, S., J. Lloret, J. M. Jimenez and L. Parra (2016). Underwater acoustic modems. IEEE Sensors Journal, 16, 11, 4063-4071.
- Shaw, G. R. and J. Lopato (2014). Software defined radio as a solution to testing RF avionics. Proceedings of IEEE Autotestcon, 290-292.
- Shao, X. (2010). Combination of MATLAB and sound card to realize Gaussian sine wave for decoding Morse code. Proceeding of IEEE Information Management and Engineering Conference, Chengdu, Republic of China, 32-34.
- Singer, A. C., J. K. Nelson and S. S. Kozat (2009). Underwater wireless communications, signal processing for underwater acoustic communications. IEEE Communications M 47, 90-96.
- Stojanovic, M. (1996). Recent advances in high-speed underwater acoustic communications. IEEE J Oceanic Engineering 21, 125-136.
- Stojanovic, M. (1999). Underwater acoustic communication. In: Wiley Encyclopedia of Electrical and Electronics Engineering, edited by Kurzman, B., John Wiley & Sons, Inc. Publishing, New York, 1-37.
- Takinaci, A.C. and T. Taralp (2013). Prediction and simulation of broadband propeller noise. Journal of Marine Science and Technology 21(5), 538-544.
- Tsung, L. L. and C. P. Kuan (2014). The numerical study of the dynamic behavior of an underwater vehicle. Journal of Marine Science and Technology 22(2), 163-172.
- Uysal, E. (2000). DSP ile Sayısal Sualtı Haberleşme Sistem Tasarımı (Digital Underwater Communication System Design with DSP), M.Sc. Thesis, Kocaeli University, Graduate School of Natural and Applied Sciences, Electronics and Telecom. Department, Kocaeli, Turkey, unpublished. (In Turkish, with English Abstract)
- Yuh, J. and J. Nie (2000). Application of non-regressor-based adaptive control to underwater robots: experiment. Computers & Electrical Engineering 26, 169-179.
- Yagnamurthy, N. K. and H. J. Jelinek (2003). A DSP based underwater communication solution. Proceeding of OCEANS 2003, San Diego, CA, USA, 120-123.
- Yilmaz, S., M. Yakut and S. İnce (2014). Design of an Experimental Platform for Depth and Direction Control Applications. TUBITAK (The Scientific & Technological Research Council of Turkey) Project. Project No: 111E294
- You, H. E., W.L. Michael and S. C. Cheng (2014). Added Mass Computation for Control of an open-frame remotely-operated vehicle: Application using WAMIT and MATLAB. Journal of Marine Science and Technology 22,4, 405-416.
- Zhiqiang, W., X. Jiadong and L. Bin (2010). A high-speed digital underwater communication solution using electric current method. Proceeding of ICFC 2010 International Conference on Future Computer and Communication, Wuhan, Republic of China, 14-16.